ARTICLE

Innovative UVC Light (185 nm) and Radio-Frequency-Plasma Pretreatment of Nylon Surfaces at Atmospheric Pressure and Their Implications in Photocatalytic Processes

M. I. Mejía,[†] J. M. Marín,[†] G. Restrepo,[†] C. Pulgarín,[‡] E. Mielczarski,[§] J. Mielczarski,[§] I. Stolitchnov,[||] and J. Kiwi*,[‡]

Applied Physicochemical Processes Research Group, Faculty of Engineering, University of Antioquia, Street 67 53-108, AA 1226, Medellin, Colombia, Institute of Chemical Sciences and Engineering, SB, GGEC Station 6, Ecole Polytechnique Fédérale de Lausanne (EPFL), 1015 Lausanne, Switzerland, INPL/CNRS, UMR 2569 LEM, 15 Av du Charmois, 54501 Vandoeuvre les Nancy, France, and Laboratore de Ceramique, STI/IMX/LC/ EPFL, Station 12, CH-1015 Lausanne, Switzerland

ABSTRACT Innovative pretreatment by UVC light (185 nm) and by radio-frequency (RF) plasma at atmospheric pressure to functionalize the Nylon surface, increasing its bondability toward TiO_2, is reported in this study. In the case of UVC light pretreatment in air, the molar absorption coefficient of O_2/N_2 at 185 nm is very low and the air in the chamber absorbs very little light from the UVC source before reaching the Nylon sample. Nylon fabrics under RF plasma were also functionalized at atmospheric pressure because of the marked heating effect introduced in the Nylon by the RF plasma. This effect leads to intermolecular bond breaking and oxygenated surface groups in the topmost Nylon layers. Both pretreatments enhanced significantly the photocatalytic discoloration of the red-wine stain in Nylon−TiO_2 compared with samples without pretreatment. The UVC and RF methods in the absence of vacuum imply a considerable cost reduction to functionalize textile surfaces, suggesting a potential industrial application. Red-wine-stain discoloration under simulated sunlight was monitored quantitatively by diffuse-reflectance spectroscopy and by CO_2 evolution. X-ray photoelectron spectroscopy (XPS) was used to monitor the changes of the C, N, and S species on the Nylon topmost layers during the discoloration process. Significant changes in the XPS spectra of Ti 2p peaks were observed during discoloration of the wine spots. Wine stains attenuated the signal of the Ti 2p (458.4 eV) peak in the Nylon−TiO_2-stained wine sample at time zero (from now on, the time before the discoloration process). Furthermore, a decrease of the wine-related O 1s signal at 529.7 eV and N 1s signal at 399.5 eV was observed during the discoloration process, indicating an efficient catalytic decomposition of the wine pigment on Nylon−TiO_2. X-ray diffraction detected the formation of anatase on the Nylon fibers. High-resolution transmission electron microscopy shows the formation of anatase particles with sizes between 8 and 20 nm.

KEYWORDS: Nylon • discoloration • photocatalysis • RF plasma • UVC pretreatment • XPS analysis

1. INTRODUCTION

The development of fabrics with self-cleaning properties is a recent area of research with a wide potential use in the textile industry (1−10). Furthermore, TiO_2-coated fabrics have been applied in pollutant degradation and bacterial inactivation (11−13). Recently, Kiwi and co-workers have reported self-cleaning activity for a variety of fabrics on different stains (3−5, 9). The pretreatment of fibers by radio-frequency (RF) plasma, molecular weight (MW) plasma, and vacuum-UV (V-UV) radiation, leading to the formation of surface bonding/chelating groups able to bind TiO_2, is the focus of these studies. Daoud et al. have also reported the pretreatment of polyester fibers using low-temperature RF plasma in the pretreatment cavity to prepare self-cleaning textiles (2).

Nylon is an artificial fiber widely used in the textile industry. Global Nylon production was 4.37 million tons in 2007 (14−16). Asia accounts for 43% of the total world output, while North America accounts for only about 30%. Western Europe and Middle East are at a very distant third and fourth, comprising 13% and 3% respectively.

We report here the innovative surface treatment of Nylon under atmospheric pressure, leading to the discoloration of the pigments in the red-wine stains for (a) Nylon pretreated by RF plasma and (b) Nylon pretreated by UVC (185 nm) light. We describe in this study the details of the discoloration process and suggest a possible discoloration mechanism. The red wine contains several hundred pigments, but its self-cleaning proceeds under solar light in a relatively fast, almost complete and reproducible way. This is the reason why we have chosen this probe in this study. RF-plasma treatment of surfaces is traditionally carried out under vacuum. The findings of RF plasma and UVC at atmospheric pressure for

* Corresponding author. E-mail: john.kiwi@epfl.ch.
Received for review May 22, 2009 and accepted September 1, 2009
[†] University of Antioquia.
[‡] Ecole Polytechnique Fédérale de Lausanne.
[§] INPL/CNRS, UMR 2569 LEM.
[||] STI/IMX/LC/ EPFL.
DOI: 10.1021/am900348u

Published on Web 09/17/2009

the pretreatment of fibers may have an application in the production of TiO_2-modified textiles, avoiding the expensive vacuum of the traditional pretreatments.

2. EXPERIMENTAL SECTION

2.1. Materials. The Nylon samples were provided by Medellin textile industry. The finished Nylon had the additives necessary for ready use. The fabric spun was processed to a lubricated and cohesive yarn (17, 18).

2.2. TiO_2 Colloidal Synthesis. Titanium isopropoxide (97%, Aldrich Chemical Co.) was added dropwise to a 0.1 M nitric acid solution (125−750 mL) under vigorous stirring. A white slurry formed, and this slurry was heated to 80 °C and stirred for 3 h to achieve peptization (i.e., destruction of the agglomerates into primary particles with a decrease of the size). The solution was then filtered through a glass frit to remove nonpeptized agglomerates. Hydrothermal treatment of the solution in an autoclave was carried out for 12 h at 250 °C to grow the primary nanoparticles. Sedimentation occurred during the autoclaving, and the particles were redispersed by two consecutive sonications. Then the colloidal suspension was introduced in a rotary evaporator at 35 °C and 3 MPa and brought to a TiO_2 concentration of 11% (w/w).

2.3. Pretreatment of Nylon Fabrics by RF Plasma. The molecular structure of Nylon-6,6 is $[-(NHCO)(CH_2)_4(CONH)-(CH_2)_6-]$ and is a polyamide fiber made by the condensation of hexamethylenediamine $NH_2(CH_2)_6NH_2$ (a diamine with six C atoms) and adipic acid $HOOC(CH_2)_4COOH$ (a dicarboxylic acid with six C atoms). The Nylon fabrics were used as a support for TiO_2 because of their good flexibility, large surface, and good absorbing power. Nylon fabrics were washed twice with detergent and water for the removal of impurities and natural grease before pretreatment in a RF-plasma cavity (Harrick Scientific Corp., Pleasantville, NY; 13.56 MHz, power 100 W) for 5, 10, and 30 min at 0.1 mbar and atmospheric pressure.

Generally, for RF-plasma formation, low pressures are needed to enhance the capture length of the electrons generated in the electric field having a higher ionization potential than that of the gas. This condition allows the plasma discharge to occur in the reactor cavity. However, without vacuum as in our experiments conducted at the low RF-plasma power of 100 W, the RF pretreatment was only able to heat the Nylon, breaking intermolecular bonds (hydrogen bonds) and partially segmenting the textile fibers (19). This introduces functional groups $C-O^-$, $-COO^-$, and $-O-O^-$ on the Nylon surface in the presence of O_2(air), enabling the attachment of TiO_2 on the Nylon by (a) exchange/impregnation (20). The nanocrystals of TiO_2 bind to the Nylon by exchange with the slightly positive Ti^{4+} of TiO_2 through electrostatic attraction/chelation with the $-COO^{2-}$, $-O-O^{2-}$ negative surface groups and (b) with the introduction of additional N−H bonds, along with amine/amide-like groups made available by the local heating on the Nylon structure (21).

2.4. Pretreatment of Nylon Fabrics by V-UVC. The textile polymer surface was also functionalized by UVC irradiation using the 185 nm line (6 W) from a 25 W (254 nm + 185 nm light) low-pressure Hg lamp (Ebara Corp., Tokyo, Japan).

RF plasma at low pressure (0.1−10 Torr) in the presence of O_2 gas generates anions and cations (O^- and O^+), radicals, excited O* sates, molecular ions, and high-energy electrons in a system that is not in equilibrium. However, UVC activation having a lower energy than that of the RF plasma does not lead to cationic or anionic oxygen species, and only atomic (O) and excited oxygen (O*) species are formed by using 185 nm light. The radiant energy at 185 nm is below 241 nm (495 kJ/mol), the energy required for the reaction $O_2 \rightarrow 2O^*$ (22). The absence of cationic or anionic oxygen leads to a more uniform distribution in the activated sites on the Nylon. This, in turn, was seen to lead to a more uniform TiO_2 layer of the textile surfaces, as found by high-resolution transmission electron microscopy (HRTEM) and described in section 3.7.

Scheme 1. Cylindrical Pyrex Photoreactor Provided with a Septum To Monitor the CO_2 Produced during the Discoloration of Stains

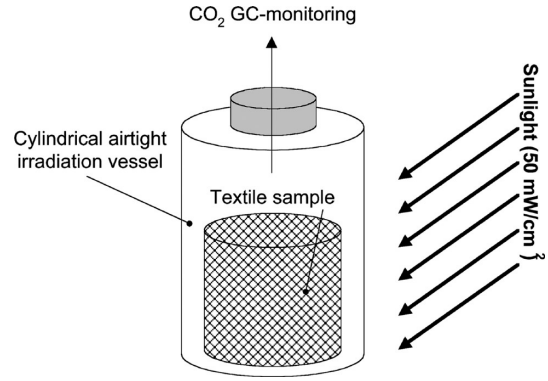

In the UVC cavity, the distance between the Nylon samples and the cylindrical UVC light was ~3 mm. The O_2 cross section is 10^{-20} cm^2, and the molar absorption coefficient ϵ_{O_2}(185 nm) $\approx 2.6\ M^{-1}\ cm^{-1}$ (22). The cross section of N_2 is about 10 times smaller than that for O_2 at this wavelength. Therefore, ϵ_{N_2}(185 nm) would negligible. At 185 nm, the extinction coefficients of O_2 and N_2 are so low that practically no UVC radiation is lost in the optical pathway between the light source and the Nylon sample even at atmospheric pressures.

2.5. Nylon Used as a Support for TiO_2. *Coating of TiO_2.* After functionalization of the textile surfaces by both RF-plasma and UVC pretreatment, the fabrics were immersed in TiO_2 colloidal solutions and impregnated/exchanged for 30 min. Afterward, the samples were dried in two steps: (a) first in air for 24 h at room temperature and (b) then by heating at 100 °C for 15 min. The samples were immersed immediately after pretreatment because the functional groups introduced at the fabric surface deactivate with time by reacting with the humidity and O_2 of the air (3). The samples were then washed with distilled water to remove TiO_2 particles that did not attach to the Nylon surface.

2.6. Evaluation of the Nylon Self-Cleaning through CO_2 Evolution. The photochemical reactors consisted of 50 mL cylindrical Pyrex flasks containing strips of TiO_2-coated textiles (9 cm^2) positioned immediately behind the reactor wall (Scheme 1). The red-wine stains were introduced on the Nylon fabric using a 70 μL microsyringe. The irradiation of the samples was carried out in a Suntest solar simulator CPS (Atlas GmbH) equipped with a Xe lamp (830 W). The solar cavity has a spectral distribution with 0.5% of the photons at wavelengths <300 nm and 7% between 300 and 400 nm. The emission spectrum between 400 and 800 nm followed the solar spectrum. The internal walls of the Suntest were of Al reflective material to conduct all of the lamp irradiation to the Pyrex vessels. The CO_2 produced during irradiation was measured in a gas chromatograph (Carlo Erba, Milano, Italy) provided with a Poropak S column.

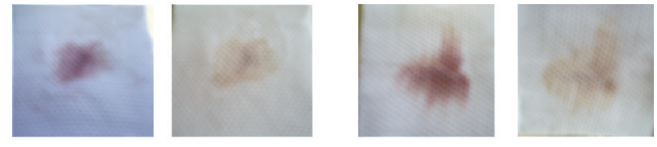

FIGURE 1. Discoloration of wine stains on Nylon−TiO_2: pretreated by RF atmospheric pressure for 30 min (a) before and (b) after 24 h of Suntest irradiation and pretreated by UVC in vacuum for 30 min (c) before and (d) after 24 h of Suntest irradiation.

Table 1. Surface Atomic Concentration in % Nylon Determined by XPS

		O						N			C						
sample	O	530	531	532	533	Ti	Ti pos	N	399.5	401.5	C	284.6	285.8	287.6	288.7	S	Si	K
nylon ref	12.23		*20.42*	*42.9*	*36.68*	0		3.66	*100.00*		83.69	*76.25*	*14.58*	*6.43*	*2.74*	0	0.4	
nylon + TiO_2 ($t = 0$)	18.75	*19.7*	*53.27*	*34.27*	*10.76*	1.71	*458.41*	4.86	*100.00*		74.68	*60.8*	*26.8*	*6.17*	*5.69*	0		
nylon + TiO_2 + wine ($t = 0$)	24.29	*0.93*	*17.51*	*53.18*	*28.37*	0.16	*458.52*	1.90	*68.19*	*31.81*	72.92	*50.9*	*42.18*	*4.36*	*2.55*	0.33	0.1	0.28
nylon + TiO_2 + wine ($t = 3$ h)	23.65	*6.77*	*22.69*	*51.55*	*19.00*	0.58	*458.42*	2.09	*57.00*	*43.00*	73.15	*54.62*	*37.83*	*4.10*	*3.45*	0.25		0.27
nylon + TiO_2 + wine ($t = 6$ h)	26.24	*11.75*	*25.76*	*48.93*	*13.56*	1.47	*458.41*	2.27	*55.46*	*44.54*	69.46	*59.61*	*28.67*	*9.39*	*2.12*	0.21		0.36
nylon + TiO_2 + wine ($t = 24$ h)	26.04	*8.14*	*29.61*	*49.00*	*13.26*	0.85	*458.43*	2.48	*66.17*	*33.83*	69.88	*54.78*	*34.75*	*4.26*	*6.20*	0.27		0.49

2.7. X-ray Photoelectron Spectroscopy (XPS). An AXIS NOVA photoelectron spectrometer (Kratos Analytical, Manchester, U.K.) equipped with a monochromatic Al Kα ($h\nu = 1486.6$ eV) anode was used in the study. The kinetic energy of the photoelectrons was determined with the hemispheric analyzer set to a pass energy of 160 eV for wide-scan spectra and 20 eV for the case of HRTEM spectra. The electrostatic charge effect of the sample was overcompensated for by means of the low-energy electron source working in combination with a magnetic immersion lens. The C 1s line with its position at 284.6 eV was used as a reference to correct the charging effect. Quantitative elemental compositions were determined from peak areas using experimentally determined sensitivity factors and a spectrometer transmission function. The spectrum background was subtracted according to Shirley (23). The HRTEM spectra were analyzed by means of spectral deconvolution software (Vision 2, Kratos Analytical, London, U.K.) (24).

2.8. Diffuse-Reflectance Spectroscopy (DRS). DRS spectra were measured using a Cary 5 UV−vis−near-IR spectrophotometer equipped with an integration sphere. Measurements were carried out on 2.5 × 2.5 cm size samples.

2.9. X-ray Diffraction (XRD) Measurements of Nylon−TiO_2. The crystallinity and phase of TiO_2 loaded on the fabric surface were studied with a Siemens X-ray diffractometer using Cu Kα radiation.

2.10. HRTEM of Nylon−TiO_2 Samples. A Philips CM 300 (field-emission gun, 300 kV, 0.17 nm resolution) high-resolution transmission electron microscope and a Philips EM 430 (300 kV, LaB_6, 0.23 nm resolution) were used to measure the particle sizes of the TiO_2 cluster coatings on the Nylon. The textiles were embedded in an epoxy resin (Embed 812), and the fabrics were cross-sectioned with an ultramicrotome (Ultracut E) to a thin section of 50−70 nm. Magnification from about 3000× to 41 000× was used to characterize the samples and determine the TiO_2 cluster size.

2.11. X-ray Fluorescence Determination of the Ti Content on the Nylon Surface. The Ti content on Nylon fabrics was evaluated by X-ray fluorescence in a PANalytical PW2400, RFX spectrometer. In this technique, each element emits an X-ray of a certain wavelength associated with its particular atomic number. The Nylon fabric before coating showed 0.36 % (w/w) Ti because of TiO_2 added during the Nylon manufacturing process. The Ti content of the Nylon samples pretreated by RF and loaded as described in section 2.5 was ∼0.99 ± 0.01 % (w/w) and was conserved throughout the discoloration process.

3. RESULTS AND DISCUSSION

3.1. Discoloration of Red-Wine Stains on TiO_2-Coated Nylon Fabrics. Parts a and b and parts c and d of Figure 1 show the red-wine-stain disappearance on pretreated Nylon by RF and UV before the reaction and after 24 h of Suntest irradiation. The samples pretreated by RF show a higher degree of discoloration than the samples pretreated by UV.

3.2. XPS of TiO_2-Loaded Nylon within the Wine-Stain Photodegradation Time. Table 1 shows a value of 1.71 % for the Ti content for Nylon−TiO_2 at time zero (before the reaction). This value decreases after wine is added, covers the Nylon topmost layers, and regains the initial value after 6 h, when TiO_2 appears again on the Nylon

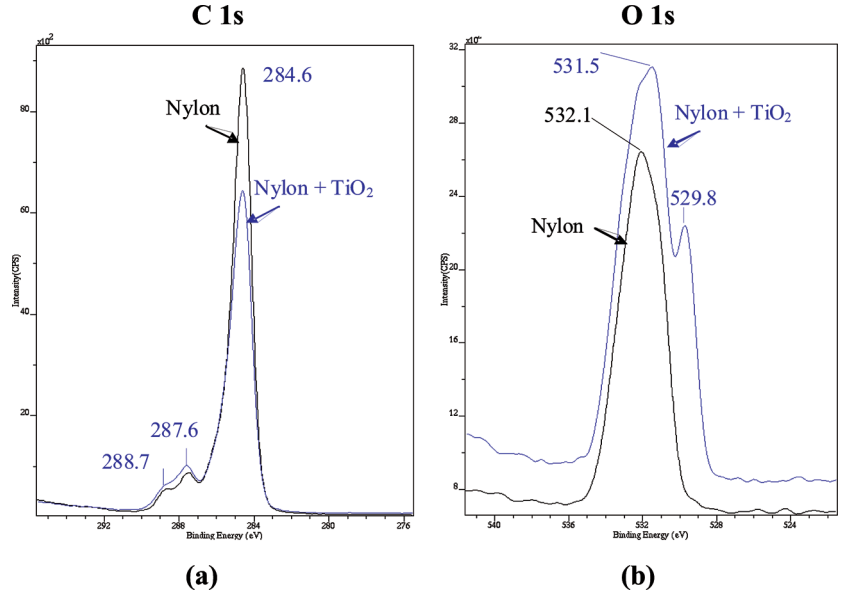

FIGURE 2. XPS spectra of Nylon fabric showing (a) the C 1s peak and (b) the O 1s peak.

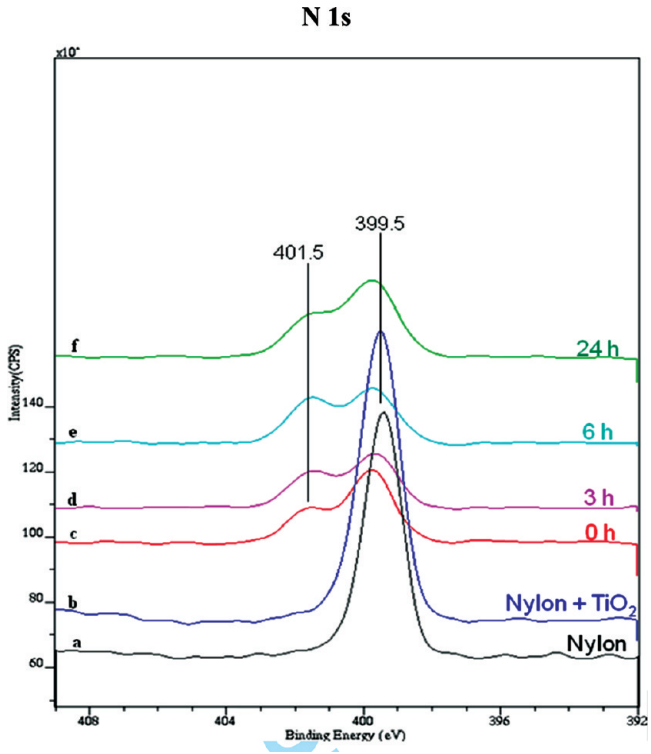

FIGURE 3. XPS spectra of N 1s peaks of (a) Nylon fabric and (b) Nylon−TiO_2 without wine at 0 h and wine-stained under Suntest light at (c) 0 h, (d) 3 h, (e) 6 h, (f) and 24 h.

surface after wine discoloration. The lower value after 24 h is lower because of the inhomogeneous TiO_2−nanoparticle coverage of the Nylon surface on the different samples. The C content of the topmost layers decreases because of two factors: (a) upon addition of the red wine at time zero and (b) during the subsequent discoloration time because of mineralization of the wine spot added. The O content values increase at time zero when TiO_2 is added to the Nylon sample because of the O content of TiO_2, and the S content due to the wine addition is seen to partially decrease during the discoloration time. The N content of the Nylon polyamide decreases after the addition of wine at time zero and regains a concentration close to the initial one after 24 h when the red wine has been partially eliminated.

Figure 2a shows the characteristic XPS C 1s peaks at 284.6, 285.8, 287.5, and 288.7 eV due to the presence of C−C, CNH(C═O), C═O, and NC═O (25−28). This is consistent with the elements found in the formulation of Nylon as stated in section 2.3. The O 1s peak for the Nylon surface alone is seen in Figure 2b at 532.1 eV. For the TiO_2-coated Nylon, the O 1s peak is observed with a binding energy (BE) of 529.8 eV due to the formation of the O−Ti^{4+} species (29, 30) on the Nylon surface. The N 1s peak at 529.8 eV of the amine group RNH_2 is also shown in Figure 2b (26).

Figure 3 presents the dynamic of the topmost-layer N peaks at different times within the 24 h discoloration time. The N peak for the higher N 1s component at 401.5 eV appears after the addition of wine (Figure 5c). This signal is assigned to quaternary N from the flavin pigment, found in red wine (31−34). The main N peak at 399.5 eV in Nylon−TiO_2 is almost constant.

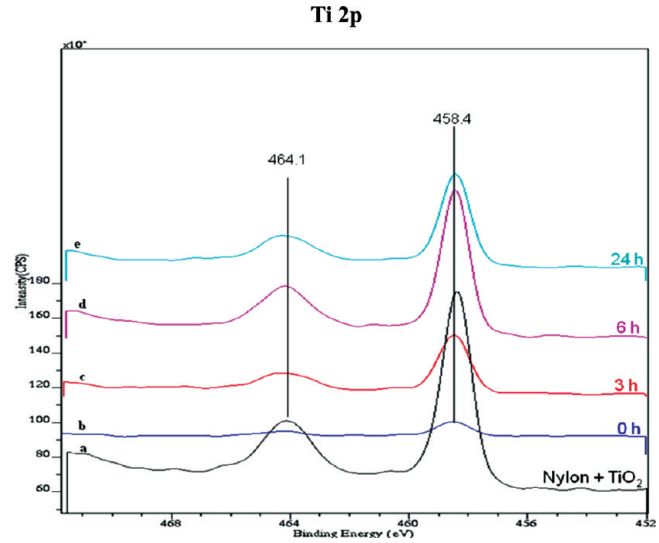

FIGURE 4. XPS spectra of Ti 2p peaks of (a) Nylon−TiO_2 without wine at 0 h and of wine-stained Nylon under Suntest light for (b) 0 h, (c) 3 h, (d) 6 h, (e) and 24 h.

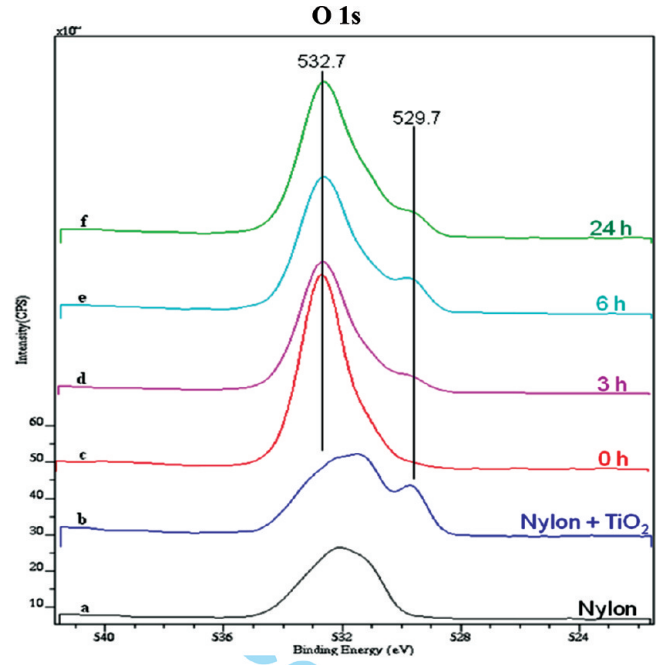

FIGURE 5. XPS spectra of O 1s peaks of (a) Nylon fabric and (b) Nylon−TiO_2 without wine at 0 h and of wine-stained Nylon−TiO_2 under Suntest light at (c) 0 h, (d) 3 h, (e) 6 h, (f) and 24 h.

A deposit of about 2% TiO_2 was found on the Nylon surface after TiO_2 coating (Ti 2p at 458.4 eV), lowering in Figure 4 other XPS signals from the Nylon. The addition of a wine spot attenuates the signal from the Nylon−TiO_2 sample at time zero, as seen in the lower peak at 458.4 eV in Figure 4. During the course of photodiscoloration, the removal of the wine spot is shown in Table 1 by a decrease of the surface C on the Nylon topmost layers. Figure 4 shows that, after 3 and 6 h, the Ti 2p signals again reached the initial intensity.

Figures 5 and 6 show by inspection of the XPS lines of C 1s, O 1s, and S 2p that wine spot removal during discoloration presents the following features: (a) The C 1s line in Figure 6 presents a higher intensity ratio between the peak

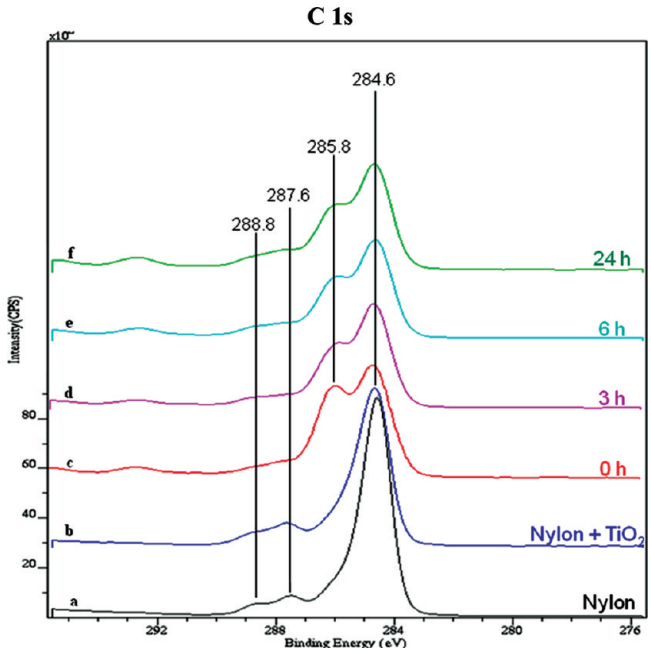

FIGURE 6. XPS spectra of C 1s peaks of (a) Nylon fabric and (b) Nylon−TiO_2 without wine at 0 h and of wine-stained Nylon−TiO_2 under Suntest light at (c) 0 h, (d) 3 h, (e) 6 h, (f) and 24 h.

components at 285.8 eV (C−O) and 284.6 eV (C−C) with reaction time. More oxidized C intermediates were observed on the Nylon as the reaction progresses. (b) The value of the O 1s component at 285.8 eV increases when the wine stain is added (see Table 1). (c) The S 2p line in the XPS spectrum (not shown) at zero reaction time shows two S components at 168.0 eV of SO_4^{2-} groups and at 163.5 eV characteristic of the S^{2-} molecular group. The sulfide (S^{2-}) was oxidized during discoloration to SO_4^{2-}, and the sulfate component increased at longer reaction times.

3.3. DRS of Wine-Stain Discoloration on Nylon−TiO_2. The DRS spectra of Nylon−TiO_2 pretreated by RF and stained with red wine are shown in Figure 7 (trace a) before Sunlight irradiation. Two absorption ranges are observed. Below 390 nm, the absorption was due to TiO_2, and above 390 nm, the absorption in the visible was due to the red-wine stain. After 24 h of Suntest light irradiation, a sharp increase in the reflectance is observed because of the red-wine discoloration [Figure 7 (trace b)].

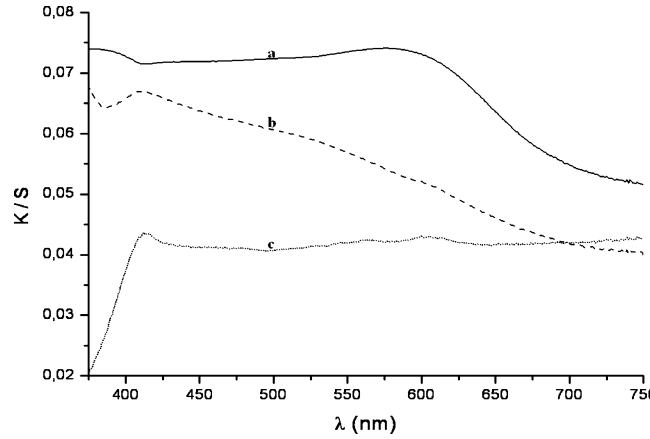

FIGURE 8. Kubelka−Munk relationships of (a) Nylon−TiO_2 stained with wine before irradiation, (b) Nylon−TiO_2 stained with wine after 24 h of Suntest irradiation, and (c) Nylon fabric alone.

The Kubelka−Munk (K/S) relations were used to transform the reflectance shown in Figure 7 data into absorption data and are presented next in Figure 8 (30). The DRS is related to the absorbance by the K/S relation using the Kubelka−Munk relation (eq 1, where S is the scattering term and R is the reflectance term.

$$\frac{K}{S} = \frac{(1 - R_\infty)^2}{2R_\infty} \equiv F(R_\infty) \qquad (1)$$

Figure 8 (trace a) shows K/S for the red-wine stain on Nylon−TiO_2 before light irradiation with an absorption shoulder between 425 and 590 nm due to the tannin,

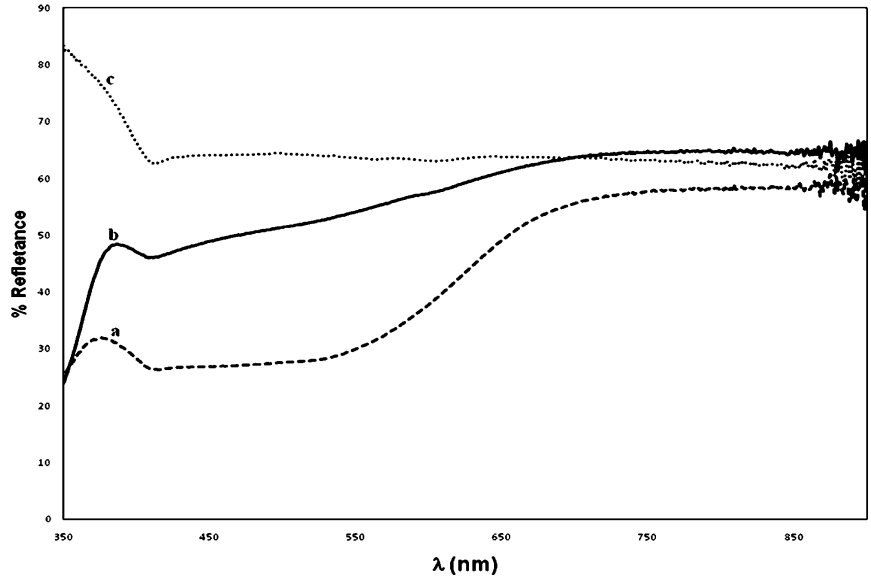

FIGURE 7. DRS spectra of (a) Nylon−TiO_2 stained with wine before irradiation, (b) Nylon−TiO_2 stained with wine after 24 h of Suntest irradiation, and (c) Nylon fabric alone.

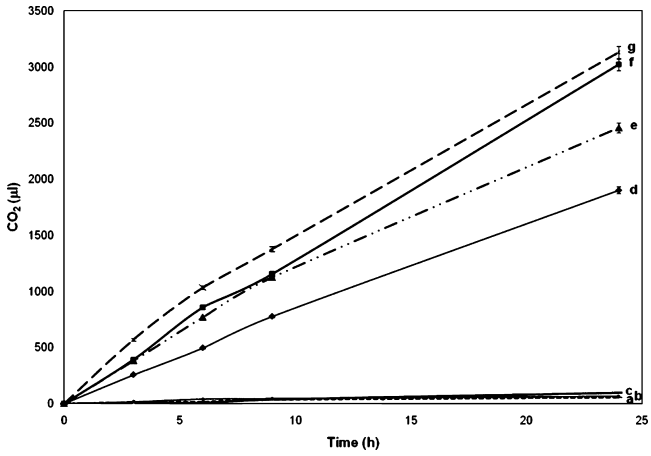

FIGURE 9. CO_2 evolution under Suntest light irradiation for UVC-pretreated samples of (a) Nylon + TiO_2 without pretreatment, (b) Nylon alone, (c) Nylon + wine stain, (d) Nylon pretreated by UVC, no vacuum during 30 min + wine stain, (e) Nylon pretreated by UV without vacuum 10 min + wine stain, (f) Nylon pretreated by V-UVC at 0.1 mbar during 30 min + wine stain, and (g) Nylon pretreated by V-UVC at 0.1 mbar during 10 min + wine stain.

carotene, porphyrin, and flavin pigments of red wine (35). Furthermore, the absorption of Nylon is seen in Figure 8 (trace c). *K*/*S* showing a decrease in the absorbance of the red-wine stain after 24 h of Suntest irradiation is presented in Figure 8 (trace b). The considerably lower values for *K*/*S* for Nylon are found in Figure 8 (trace c).

3.4. CO_2 Evolution during Wine-Stain Discoloration on Nylon−TiO_2. ***3.4.1. CO_2 Evolution of Nylon−TiO_2 Pretreated by UVC with and without Vacuum.*** Wine stains are mineralized under Suntest irradiation, leading to CO_2.

$$C_xH_yN_zS_w + H_2O_v + O_2(\text{air}) \rightarrow CO_2 + SO_p + NO_q + H_2O \quad (2)$$

CO_2 evolution during discoloration of wine-stained Nylon and Nylon−TiO_2 samples pretreated by UVC light is shown in Figure 9. It can be seen that samples pretreated by UVC for 10 min at 0.1 mbar (Figure 9, trace g) show the highest CO_2 evolution (3532 μL) after 24 h of irradiation. Samples pretreated by V-UVC for 30 min (Figure 9, trace f) at 0.1 mbar produced the second highest amount of CO_2 (2607 μL). Samples with UVC pretreatment at atmospheric pressure (Figure 9, trace e) produced 2353 μL of CO_2 after 24 h of irradiation. This result in the absence of vacuum makes UVC highly convenient for industrial applications, reducing cost because no vacuum is required. Very small amounts of CO_2 were found for Nylon fabrics stained with red wine in the absence of TiO_2 (trace c) and for Nylon irradiated in the absence of TiO_2 and wine (trace b).

3.4.2. CO_2 Evolution of Nylon Fabrics Pretreated by RF Plasma with and without Vacuum. Figure 10 shows the evolution of CO_2 during red-wine-stain discoloration as a function of the irradiation time for samples of Nylon and Nylon−TiO_2 pretreated by RF plasma. Samples pretreated by RF plasma without vacuum for 10 min (Figure 10, trace g) produced the highest amount of CO_2 (3131 μL) after 24 h. Samples pretreated by RF plasma without vacuum for 30 min (Figure 10, trace f) showed CO_2 production slightly lower than that of the previous sample. This suggests that 10 min is the optimum time for the pretreatment of Nylon fabrics by RF/no vacuum. Pretreatment of Nylon−TiO_2 samples for longer times only led to additional cost without increasing the amount of CO_2 evolved from the sample.

Furthermore, the amount of CO_2 released by samples pretreated by RF with vacuum (traces f and d) was lower than that achieved without vacuum, showing that RF without vacuum enhances stain degradation. Only small amounts of CO_2 (63 μL) were observed when Nylon was irradiated in the Suntest (Figure 10, trace b). Also, only small amounts of CO_2 (96 μL) were found for Nylon stained with wine in the absence of TiO_2 (Figure 10, trace c).

The reproducibility observed for CO_2 mineralization was established by running three different samples of Nylon−TiO_2 pretreated by RF and UVC and stained with the same amount of red wine. The amount of CO_2 evolved showed a reproducibility of 2% during our experimental measurements. Generally, RF-plasma and UVC pretreatment induced localized heating in the Nylon breaking of intermolecular bonds (hydrogen bonds), partially segmenting the textile and introducing functional groups −C−O−, −OOH, −O−C═O, −O−O^-, and −COO^- on the Nylon, in the presence of O_2(air). The amount of functional groups cannot be quantified by XPS or other techniques. It seems to be higher in the case of UVC (Figure 9) than in the case of RF plasma (Figure 10) because a higher amount of CO_2 was evolved from the wine stain during photocatalysis. This may be due to a higher amount of TiO_2 attached on the functionalized Nylon surface by exchange/impregnation as described in section 2.3.

3.5. XRD of Nylon−TiO_2. The XRD patterns of Nylon textile before and after TiO_2 loading by RF pretreatment for a sample pretreated in vacuum for 10 min are shown in Figure 11. The XRD spectra confirmed a TiO_2 anatase phase on the Nylon (trace 1). This result is consistent with the XPS observation shown in Figure 4. The peaks at 20.32°, 21.36°, and 23.8° in traces 1 and 2 come from the Nylon substrate. The Brookite orthorhombic TiO_2 phase shows a strong peak at around 31° (precisely at 30.81°, as shown in the TiO_2 database). Hence, this small peak at 31° in Figure 11 could be due to the presence of a small quantity of Brookite.

3.6. HRTEM on Nylon−TiO_2. Figure 12 shows an almost continuous coating of TiO_2 on the Nylon surface at time zero. The thickness of the TiO_2 layer was found to be between 35 and 115 nm and was maintained after the 24 h discoloration process. The TiO_2 particle sizes from 8 to 20 nm determined by HRTEM are shown in Figure 13. This TiO_2 particle size was small enough to render transparent films and keep the original handling touch of the Nylon. This is important for the potential application of Nylon−TiO_2 self-cleaning fabrics. No atomic force microscopy could be

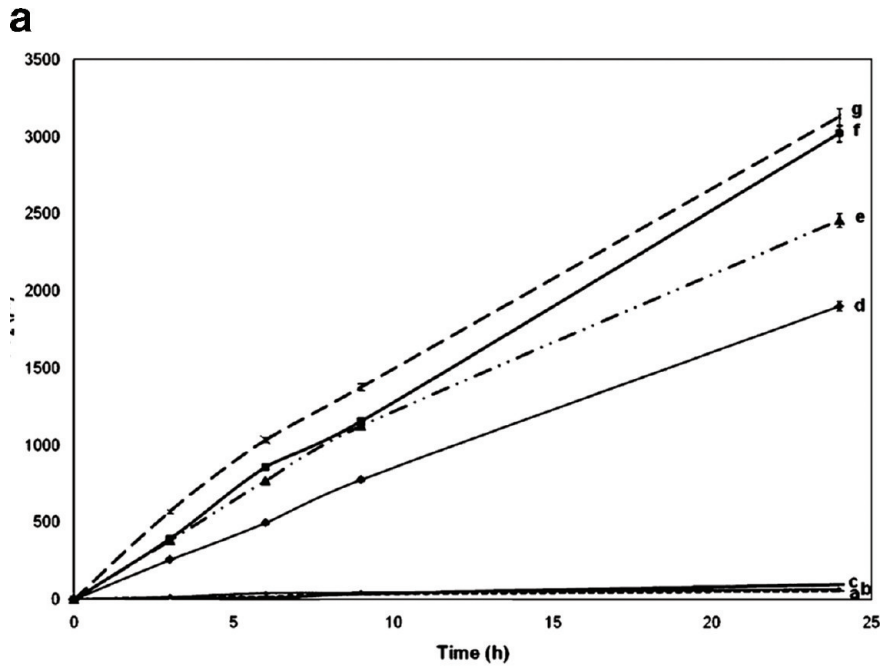

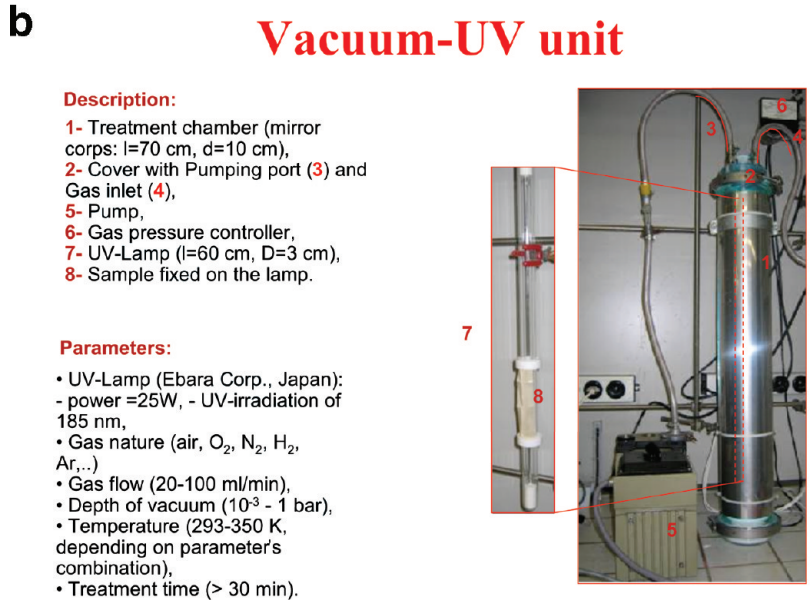

FIGURE 10. (Part a) CO_2 evolution under Suntest light irradiation for RF-pretreated samples of (a) Nylon + TiO_2 without pretreatment, (b) Nylon alone, (c) Nylon + wine stain, (d) Nylon pretreated by RF plasma, 0.1 mbar, during 30 min + wine stain, (e) Nylon pretreated by RF plasma at 0.1 mbar during 10 min + wine stain, (f) Nylon pretreated by RF plasma without vacuum during 30 min + wine stain, and (g) Nylon pretreated by RF plasma without vacuum for 10 min + wine stain. (Part b) Schematic of the V-UVC unit.

carried out on these samples because of rough nonhomogeneous surface of Nylon−TiO_2.

4. CONCLUSIONS

(i) Two innovative pretreatments of the Nylon surface are presented: (a) RF plasma at atmospheric pressure was able to bind TiO_2 because of the heat effect introducing hydrocarbon chain scission and oxygenated functionalities in the Nylon chains, and (b) UVC light (185 nm) at atmospheric pressure led to the formation of atomic O and excited O* in the gas phase because of the extremely low optical molecular absorption of O_2 and N_2 at 185 nm.

(ii) Although samples pretreated by V-UVC for 10 min exhibited the most favorable CO_2 evolution under Suntest light, the samples pretreated by RF under atmospheric pressure reached a comparable level of CO_2 formation. Therefore, the absence of vacuum makes the pretreatment presented in this study promising for the surface activation of fibers.

(iii) High-reproducibility stain discoloration was observed for RF plasma and UVC under Suntest light.

(iv) Anatase TiO_2 particles were bonded on Nylon in a stable manner. These particles did not show any modification after repeated red-wine discoloration cycles.

Acknowledgment. The authors thank COLCIENCIAS and the University of Antioquia, Medellin, and COST Action 540 PHONASUM "Photocatalytic technologies and novel nano-

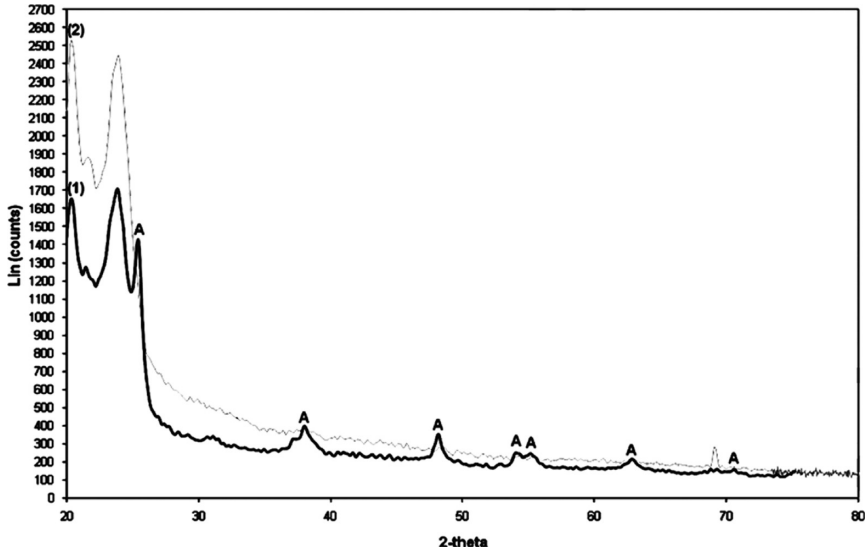

FIGURE 11. XRD patterns of (1) Nylon fabric and (2) Nylon−TiO_2 pretreated by RF plasma for 10 min (A stands for the anatase crystallographic form).

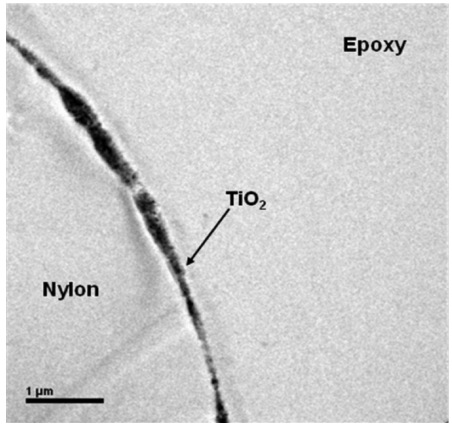

FIGURE 12. TEM of a Nylon−TiO_2 fabric at time zero.

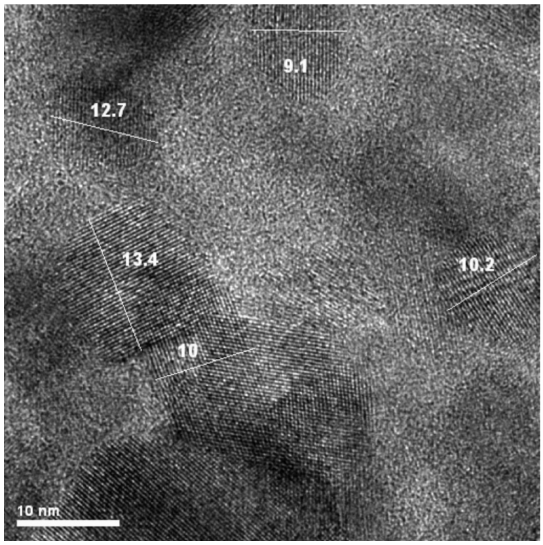

FIGURE 13. HRTEM of Nylon−TiO_2 at time zero showing the TiO_2 clusters and atomic planes (scale of 10 nm).

surafce materials, critical issues", Bern, for financial support. We are thankful for the help of J.-M. Lavanchy (IMG-Centre d'Analyse Minerale, Bat Anthropole, University of Lausanne, CH-1025, Lausanne, Switzerland) with the X-ray fluorescence and of Y. Arroyo (CIME-EPFL, Bat MXC-134, Station 12, 1015 Lausanne, Switzerland) with the electron microscopy work.

REFERENCES AND NOTES

(1) Yuranova, T.; Laub, D.; Kiwi, J. *Catal. Today* **2007**, *122*, 109–117.
(2) Qi, K.; Xin, J.; Daoud, A. W. *Int. J. Appl. Ceram. Technol.* **2007**, *4*, 554–563.
(3) Bozzi, A.; Yuranova, T.; Kiwi, T. *J. Photochem. Photobiol. A* **2005**, *172*, 27–34.
(4) Bozzi, A.; Yuranova, T.; Guasaquillo, I.; Laub, D.; Kiwi, T. *J. Photochem. Photobiol. A* **2005**, *174*, 156–164.
(5) Meilert, K.; Laub, D.; Kiwi, J. *J. Mol. Catal. A: Chem.* **2005**, *237*, 101–108.
(6) Tung, W.; Daoud, A. W. *J. Colloid Interface Sci.* **2008**, *326*, 283–288.
(7) Uddin, M.; Cesano, F.; Scarano, D.; Bonino, F.; Agostini, G.; Spoto, G.; Bordiga, S.; Zecchina, A. *J. Photochem. Photobiol. A* **2008**, *199*, 64–72.
(8) Liuxue, Z.; Xiulian, W.; Peng, L.; Zhixing, S. *Surf. Coat. Technol.* **2007**, *201*, 7607–7614.
(9) Yuranova, T.; Mosteo, R.; Bandara, J.; Laub, D.; Kiwi, J. *J. Mol. Catal. A: Chem.* **2006**, *244*, 160–167.
(10) Bitlisli, B.; Yumurtas, A. *J. Soc. Leather Technol. Chemists* **2008**, *92*, 183–186.
(11) Yuranova, T.; Rincón, G.; Bozzi, A.; Parra, S.; Pulgarin, C.; Albers, P.; Kiwi, J. *J. Photochem. Photobiol. A* **2003**, *161*, 27–34.
(12) Kangwansupamonkon, W.; Lauruengtana, V.; Surassmo, S.; Ruktanonchai, U. *Nanomed.: Nanotechnol., Biol., Med.* doi: 10.1016/j.nano.2008.09.004, in press.
(13) Yuranova, T.; Rincon, A.; Pulgarin, C.; Laub, D.; Xanthopoulos, N.; Mathieu, H.; Kiwi, J. *J. Photochem. Photobiol. A* **2006**, *181*, 363–369.
(14) Kin-Fan, F.; Man-Chong, C. *J. Asia Textile Apparel* **2007**, *20*, 152–156.
(15) Global Reports, Yarns and Fibers Exchange. *Nylon Chain Report 2008*; Dec 24, **2008**.
(16) Chan, C.; Ko, T.; Hiroaka, H. *Surf. Sci. Rep.* **1996**, *24*, 1–54.
(17) Mejía, M.; Marín, J.; Restrepo, G.; Ríos, L. *Rev. Sci Techn.* **2007**, *36*, 97–102.
(18) Gallardo, E. Accessed Jan 2006, http://gallardo.20m.com/cap08.htm.
(19) Johnson, A. *The Theory of Coloration of Textiles*; Society of Dyers and Colourists: Bradford, U.K., 1989.
(20) Dhananjeyan, M.; Kiwi, J.; Thampi, R. *Chem. Commun.* **2000**, 1443–1444.
(21) Willert-Porada, M. Advances in microwave and radio frequency processing. *Report from the 8th International Conference on Mi-*

crowave and High-Frequency Heating, Bayreuth, Germany, Sept 3−7, 2001; Springer: Berlin, 2001; pp 440−443.
(22) *Handbook of Chemistry and Physics*; CRC Publishing Co.: Boca Raton, FL, 2004.
(23) Shirley, D. A. *Phys. Rev. B* **1972**, *5*, 4709–4716.
(24) Briggs, D.; Shea, M. *Practical Surface Analysis: By Auger and X-Ray Photoelectron Spectroscopy*, 2nd ed.; John Wiley and Sons: New York, 1990.
(25) Upadhyay, D.; Cui, N.; Anderson, C.; Brown, D. *Colloids Surf., A* **2004**, *248*, 47–56.
(26) Fu, R.; Cheung, I.; Mei, Y.; Shek, C.; Siu; Chu, P.; Huang, X.; Yang, S. *Nucl. Instrum. Methods Phys. Res. B* **2005**, *237*, 417–421.
(27) Pappas, D.; Bujanda, A.; Demaree, J.; Hirvonen, K.; McKnight, S. *Surf. Coat. Technol.* **2006**, *201*, 4384–4388.
(28) Cui, N.; Upadhyay, D.; Anderson, A.; Brown, D. *Surf. Coat. Technol.* **2005**, *192*, 94–100.
(29) Hidalgo, M.; Aguilar, M.; Maicu, M.; Navío, J. A.; Colón, G. *Catal. Today* **2007**, *129*, 50–58.
(30) Rengifo-Herrera, J.; Mielczarski, E.; Mielczarski, J.; Castillo, N.; Kiwi, J.; Pulgarin, C. *Appl. Catal. B* **2008**, *84*, 448–456.
(31) Geng, W.; Kumabe, Y.; Nakajima, T.; Ohki, A. *Fuel* **2009**, *88*, 644–649.
(32) Schmiers, H.; Friebel, H.; Streubel, P.; Hesse, R.; Köpsel, R. *Carbon* **1999**, *37*, 1965–1978.
(33) Carmen, S. *Bull. USAMV-CN* **2007**, 63–64.
(34) Massey, V. *Biochem. Soc. Trans.* **2000**, *28*, 2430.
(35) Bakker, J.; Timberlake, C. *J. Agric. Food Chem.* **1997**, *45*, 35–43.

AM900348U